ASD TECHNICAL REPORT 61-171 (III)

FLIGHT SIMULATION OF ORBITAL AND REENTRY VEHICLES

PART III — AERODYNAMICS INFORMATION REQUIRED FOR SIX DEGREES OF FREEDOM SIMULATION

H. BUNING

THE UNIVERSITY OF MICHIGAN

DECEMBER 1961

Contract Monitor: L. J. Kummeth
Contract No. AF 33(616)-5664
Project No. 6114
Task No. 611407

BEHAVIORAL SCIENCES LABORATORY
AEROSPACE MEDICAL RESEARCH LABORATORIES
AERONAUTICAL SYSTEMS DIVISION
AIR FORCE SYSTEMS COMMAND
UNITED STATES AIR FORCE
WRIGHT-PATTERSON AIR FORCE BASE, OHIO

1000 - August 1962 - 43-1930 & 1931

FOREWORD

The research on which this report is based was performed by the Aeronautical and Astronautical Engineering Department of The University of Michigan, Ann Arbor, Michigan, under Air Force Contract AF 33(616)-5664, Project No. 6114, "Training Equipment, Simulators, and Techniques for Air Force Systems," and Task No. 611407, "Mathematical Models." Professors G. Isakson and R. M. Howe directed the research for The University of Michigan. Mr. L. J. Kummeth of the Simulation Techniques Section, Training Psychology Branch, Behavorial Sciences Laboratory, Aerospace Medical Research Laboratories, was project engineer for the Aeronautical Systems Division.

This report is Part III of a series of several parts under the general title, "Flight Simulation of Orbital and Reentry Vehicles." Research covered in it began June 1960 and was completed in November 1961.

ABSTRACT

A survey of the aerodynamic information required for a simulator for a glide reentry vehicle is presented. Various phases of the flight are considered: hypersonic reentry, hypersonic-supersonic glide, and supersonic-transonic-subsonic approach and landing. Accuracy requirements and origin of aerodynamic information are briefly discussed.

Aerodynamic parameters are defined, and the dependence of aerodynamic coefficients on these parameters is outlined.

Special emphasis is placed on a technique for generating functions of two or three independent variables and some sample calculations are presented.

PUBLICATION REVIEW

Walter F. Grether

WALTER F. GRETHER
Technical Director
Behavioral Sciences Laboratory
Aerospace Medical Research Laboratories

TABLE OF CONTENTS

LIST OF SYMBOLS

a	speed of sound, ft/sec.
a, $\bar{a}$	auxiliary functions, Chapter 4
α	angle of attack
b, $\bar{b}$	auxiliary functions, Chapter 4
β	angle of sideslip
C	(with suitable subscript) aerodynamic coefficient
D	drag force (lb)
δ_a, δ_e, δ_r	aileron, elevator and rudder deflection
F_x, F_y, F_z	body axes components of resultant aerodynamic force
γ	ratio of specific heats
L, M, N	body axes components of resultant aerodynamic moment
L	lift force (lb)
ℓ	characteristic length
M	Mach number
μ	coefficient of viscosity, slug/ft sec.
q	dynamic pressure lb/ft^2
p, q, r	angular velocity components in body axes
R	gas constant for air, ft lb/slug ^oR
R_e	Reynold's number
ρ	air density, $slug/ft^3$
S	wing area, ft^2
T	absolute temperature, ^oR
$\bar{v}_a$	relative velocity vector between vehicle and surrounding air
V_a	absolute value of $\bar{v}_a$
$v_{a_x}, v_{a_y}, v_{a_z}$	body axes components of $\bar{v}_a$

1. INTRODUCTION

1.1 Aerodynamic Regimes During Reentry

The successful simulation of aircraft flight behavior depends on a reasonably accurate calculation, in real time, of the aerodynamic forces and moments acting on the vehicle. This aerodynamic information is presented exclusively in the form of aerodynamic force and moment coefficients to which the corresponding forces and moments are proportional. These coefficients are in general strong functions of the vehicle profile presented to the on-rushing air, that is, the angle of attack and angle of sideslip, α and β, respectively. In addition, they are functions of the Mach number and perhaps Reynolds' number, although the dependence on the latter aerodynamic parameter has not been investigated here.

The presentation of aerodynamic data and the subsequent generation of this information for input into analog computer equipment presents some unusual difficulties.

The Mach number range traversed in each reentry mission extends from the original entry Mach number of approximately 26 down into the subsonic range. The entire flight history of the reentry vehicle may be broken up into three phases: 1) the reentry phase between altitudes of 300,000 ft. to 200,000 ft., 2) the glide phase, between 200,000 and 100,000 ft. altitude, and 3) the approach and landing phase from 100,000 ft. down to sea level.

The first phase is characterized by hypersonic Mach numbers, that is, $M > 10$. Good estimates of aerodynamic characteristics may be made here by calculations using Newtonian flow theory. Various methods are described in ref. 6, and applied to representative bodies in ref. 7.

In this phase also the rotary derivatives, that is, the influence of angular velocity on the aerodynamic moments are negligible. These derivatives are created by the fact that various surfaces experience, in addition to the flight velocity of the vehicle, a velocity which is due to the angular velocity. This additional velocity causes a change in direction of the flow seen by these surfaces. It is clear that for very high flight velocities this effect decreases if the angular velocities are kept in the same order of magnitude.

In the absence of these derivatives the motion is essentially undamped.

The second, or glide phase, is characterized by a continuing increase in the dynamic pressure and a decrease in velocity. Although for certain reentry paths it is possible that this phase is entirely hypersonic, that is, the Mach number stays above 8.0, the minimum Mach number encountered at the end, at an altitude of 100,000 ft., is approximately 3.0. Having thus entered the supersonic range, the prediction of aerodynamic forces, moments, and

stability derivatives must rely heavily on wind tunnel tests as it does in the approach and landing phase where the flight velocity decreases through the transonic range into subsonic velocities.

At the supersonic, transonic, and subsonic flight velocities, conventional, linearized equations are likely to be satisfactory for training-type simulators. This general range, with the exception of the final landing procedure, occurs at high values of the dynamic pressure, and angle of attack and sideslip are not large.

1.2 Required Accuracy of Aerodynamic Data

The required accuracy with which the aerodynamic data and specifically the stability derivatives are fed into the simulator computer is not easy to assess. It requires considerable experience with typical solutions for the flight behavior. One approach is to study several successive solutions of the vehicle response due to standard inputs in which a particular derivative is varied by increasingly larger amounts. In this way the sensitivity of the solution to the particular stability derivative is established and used as a criterion to determine the required accuracy of this derivative. In ref. 8 Howe has suggested, on this basis, ranges of accuracy required for the stability derivatives. Similar work on specific high performance aircraft has been published in classified literature.

1.3 Availability of Aerodynamic Data

Aerodynamic data are obtained by direct computation and wind tunnel tests. The former method can be used practically for the hypersonic regime where Newtonian flow may be assumed, and the pressure coefficient has a simple relationship to the local shape of the body. Even so, such computations become rapidly quite elaborate for even simple general shapes if large ranges of angle of attack and angle of sideslip are considered.

Wind tunnel test results in the subsonic and supersonic range should be quite complete although, in general, exhaustive tests are only made at a few select values of the Mach number. As a consequence, aerodynamic data must be interpolated or "faired" between these values to obtain continuous functions of Mach number.

Data at hypersonic Mach numbers are obtained in one of several hypersonic test facilities. These tests are of extremely short duration, and the air is often contaminated with foreign substances. The aerodynamic coefficients, however, become less Mach number dependent as the Mach number increases, and approach asymptotically the values predicted by Newtonian theory at $M = \infty$.

Complete aerodynamic data for the Dynasoar glider, based on recent wind tunnel tests, will be available in the near future, ref. 9.

2. AERODYNAMIC PARAMETERS

2. 1 Introduction

Aerodynamic forces and moments are invariably proportional to the dynamic pressure while the corresponding force and moment coefficients depend to a more or less degree on the Mach number, Reynolds' number and the vehicle orientation with respect to the relative velocity vector, that is, the velocity of the vehicle relative to the surrounding atmosphere. The moments due to the rotary derivatives, i. e., the derivatives of moment coefficients with respect to angular velocities require, strictly speaking, a calculation of the angular velocity of the vehicle with respect to the surrounding atmosphere. The difference, however, between this angular velocity and the angular velocity with respect to an inertial frame of reference is at the most so small that, for the purposes of computing moments due to angular velocities, the latter may be used.

These various aerodynamic parameters are discussed below.

2. 2 Dynamic Pressure

The dynamic pressure is defined by

$$q = \frac{1}{2} \rho V_a^2 \frac{lb}{ft^2} \qquad (2.1)$$

where ρ is the atmospheric density in slug/ft^3 and V_a the absolute value of the vehicle velocity (in ft/sec) relative to the surrounding atmosphere. The major difficulty with this parameter is the large numerical range of both ρ and V_a during a typical reentry mission. The range of the dynamic pressure itself is not as large since the large values of V_a occur at the low values of ρ. This results in a numerical range of 1 - 100 for the dynamic pressure as compared to 1 - 10^6 for the density and 1 - 25 for the velocity.

Various methods are being considered to overcome these scaling difficulties. All involve a switching of scaling factors. A novel method, reported in ref. 4, involves the generation of the one-sixth power of the density, a quantity which itself has a range of 1 - 10. This is multiplied, in sequence, by V_a and twice by $\rho^{1/6}$ giving respectively $\rho^{1/6} V_a$, $\rho^{1/3} V_a$, and $\rho^{1/2} V_a$. The last quantity is then squared to yield 2q.

Various techniques of generating an approximation to the exponential density altitude variation and their effect on the results are still under investigation.

2. 3 Mach Number

The Mach number is defined by

$$M = \frac{V_a}{a} \qquad (2.2)$$

where a is the local speed of sound (ft/sec). The speed of sound depends on the altitude and specifically, is proportional to the square root of the local temperature according to:

$$a = \sqrt{\gamma R T} = 49.1 \sqrt{T} \qquad (2.3)$$

where γ is the ratio of specific heats, taken as 1.40, R is the gas constant for air and numerically equal to 1715 ft lb/slug ^{o}R, T is the air temperature in degrees Rankine.

Although the temperature varies in an irregular fashion in the range of altitudes up to 400,000 ft, the maximum variation of temperature is approximately 150^{o} (between the minimum of 354 ^{o}R at 270,000 ft and 509 ^{o}R at 170,000 ft, ref. 5). If an average, constant, temperature of 422 ^{o}R is assumed for the purposes of calculating the speed of sound, the Mach number so calculated will always be within 10% of the actual value. This assumption corresponds to the assumption of a constant speed of sound of 1008 ft/sec.

2.4 Reynolds' Number

The Reynolds' number is defined by:

$$R_e = \frac{\rho V_a \ell}{\mu} \qquad (2.4)$$

where ℓ is a characteristic length, μ the coefficient of viscosity.

The choice of the characteristic length, ℓ, depends largely on the particular physical phenomenon under consideration: the leading edge thickness of the wing to determine the heat transfer rate there, the distance along the surface or boundary layer thickness to calculate whether the flow is laminar or turbulent.

Although the effect of Reynolds' number either on aerodynamic force coefficients or on aerodynamic heating characteristics has not been considered in this report, the Reynolds' number per foot (that is, R_e/ℓ) will need to be calculated in order to determine at least surface temperature in the critical heating areas of the vehicle: fuselage nose, surface leading edges, and the lower portion of the wing surface at high values of the angle of attack.

The value of the viscosity coefficient μ does not vary radically in the altitude range considered.

2.5 Angles of Attack and Sideslip

All force and moment coefficients strongly depend on the vehicle profile presented to the on-rushing air. This profile is determined by two angles, the angle of attack α and the angle of sideslip β, which define the orientation of the relative velocity vector of the vehicle and the surrounding atmosphere in the body axes system.

If v_{a_x}, v_{a_y}, v_{a_z} are the X_B, Y_B, and Z_B components in body axes of the velocity V_a, then the angles α and β are defined as:

$$\alpha = \tan^{-1} \frac{v_{a_z}}{v_{a_x}} \tag{2.5}$$

$$\beta = \tan^{-1} \frac{v_{a_y}}{\sqrt{v_{a_x}^2 + v_{a_z}^2}} = \sin^{-1} \frac{v_{a_y}}{V_a} \tag{2.6}$$

The geometry is shown in fig. 1.

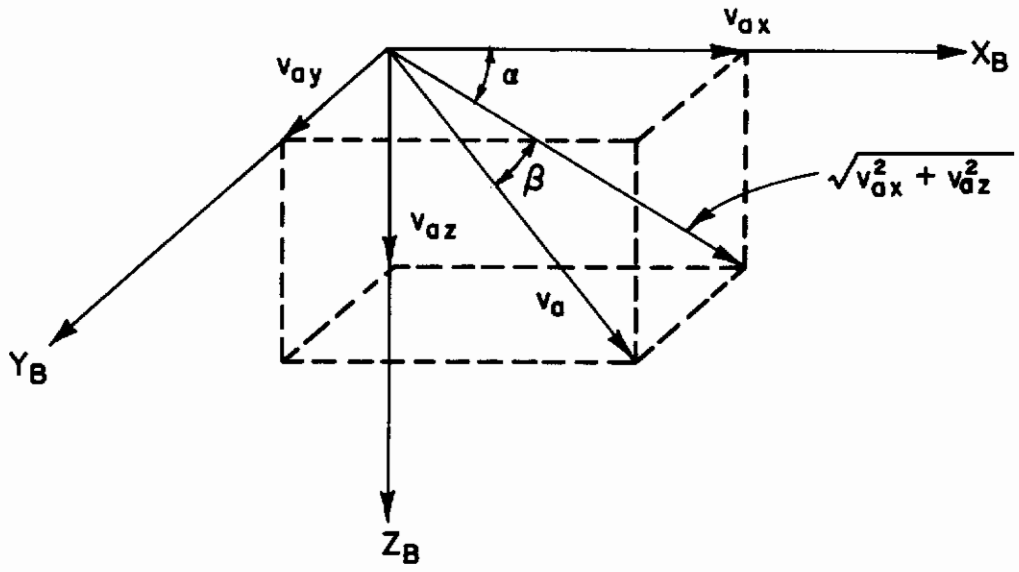

Figure 1. Definition of angle of attack, α, and angle of sideslip, β.

3. AERODYNAMIC COEFFICIENTS

3.1 Introduction

The resultant aerodynamic reaction by the atmosphere on the vehicle consists of a resultant force and a resultant moment. Aerodynamic force information is either in the form of the body axes components of this force:

$$F_x,\ F_y,\ F_z \quad \text{(lb)} \tag{3.1}$$

or in the stability axes components:

$$\mathcal{L},\ \mathcal{D},\ F_z \quad \text{(lb)} \tag{3.2}$$

where $\mathcal{L}$ is the lift, the component of the aerodynamic force in the place of symmetry of the vehicle and perpendicular to the relative velocity $\overline{v}_a$, and $\mathcal{D}$, the drag, is the component in the same plane and along the direction of the relative velocity.

In general, it is preferable to have the force information available in the axis system in which the translational equations are solved. Since neither body axes nor stability axes are found to be most suitable for the translational equations the aerodynamic force components, be it those given by equation (3.1) or by equation (3.2), must be transformed to the particular axis system selected by the use of the appropriate transformation matrix.

There is at present no uniform standard method of presenting aerodynamic data. Subsonic aerodynamic data are mostly presented in terms of lift, drag, and side force, while supersonic and hypersonic force information is usually given in body axes components.

With regard to wind tunnel data this is primarily due to a basic difference in wind tunnel instrumentation. The large subsonic tunnels in general are equipped with balance systems which measure forces in the vertical direction and along the tunnel centerline (lift and drag). Supersonic tunnels employ balance systems which are internal to the model primarily because of the considerable aerodynamic interference that would exist between external balance components and the flow over the model, and secondly, because of the space limitations imposed by the test section sizes. This last restriction is still very much felt in hypersonic test facilities. In such internal balance systems forces are measured by strain guage measurement on the supporting sting and as such measure forces normal and along the sting. Since sting and model form an integral part, the sting moves with the model as angle of attack is changed and consequently the forces measured are in body axes components.

Many wind tunnels have, however, digital read-out equipment which could well be used to compute whatever force components are desired by the user of the data. There has been considerable undecisiveness on the part of the users, however, as to what components they desire.

Most gross performance characteristics are dictated by parameters derived from the basic lift and drag forces.

The aerodynamic resultant moment is almost directly used in the form of its body axes components:

$$L,\ M,\ N \quad \text{(ft lb)} \tag{3.3}$$

since the rotary equations are invariably solved in the body axes system. If the aerodynamic moment data are presented in stability axes, and as such fed into the computer, they must first be transformed to body axes.

The force components are proportional to the non-dimensional force coefficients: C_{F_x}, C_{F_y}, and C_{F_z}. The actual forces are computed from these coefficients in a uniform manner: by multiplication with the product of dynamic pressure and a reference area (the wing area) S:

$$F = C_F \left(\frac{1}{2} \rho V_a^2\right) S \tag{3.4}$$

In a corresponding fashion the non-dimensional moment coefficients C_ℓ, C_m, C_n are defined. The actual moments are obtained from the coefficients by multiplication by the product of dynamic pressure, characteristic area, S, and a characteristic length. This characteristic length is c (some reference chord length) for the pitching moment M, and the wing span b for the rolling moment L and the yawing moment N. Hence,

$$\begin{aligned} M &= C_m \left(\frac{1}{2} \rho V_a^2\right) S\, c \\ L &= C_\ell \left(\frac{1}{2} \rho V_a^2\right) S\, b \\ N &= C_n \left(\frac{1}{2} \rho V_a^2\right) S\, b \end{aligned} \tag{3.5}$$

Calculation of the above six aerodynamic quantities is thus now tantamount to calculating the corresponding coefficients.

These coefficients and their dependence on attitude, angular velocities and control surface deflections are discussed below.

3.2 Catalog of Aerodynamic Data

In order to obtain a systematic survey of the important aerodynamic data it is convenient to construct a diagram as shown in fig. 2.

Vertically are listed the six aerodynamic coefficients discussed above. Along the top are the factors on which these coefficients depend. The coefficients are grouped in two sets of three: 1) those of importance in longitudinal characteristics: $C_{\mathcal{L}}$, $C_{\mathcal{D}}$, (or F_x, F_z) and C_m and 2) those involved in the lateral and directional aerodynamic characteristics: C_{F_y}, C_ℓ, C_n.

		Attitude Rel. to Atmosphre		Angular Vel. Components			Control Surface Deflections		
		α	β	p	q	r	δ_a	δ_e	δ_r
Longitudinal Characteristics	C_x	1 α, M						4	
	C_D	1 α, M							
	C_m	1 α, δ_e, M			2 M			3 α, M	
Directional and Lateral Characteristics	C_{Fy}		1 α, M						4
	C_ℓ		1 α, M	2 α, M		2 α, M	3 α, δ_e, M		4
	C_n		1 α, M	2 α, M		2 α, M	4		3 α, M

1. Primary functions of attitude (all regimes).
2. Primary rotary functions (unimportant in hypersonic regime).
3. Primary control effectiveness functions.
4. Secondary functions for which data available (ref. 9).

Figure 2. Schematic presentation of dependence of aerodynamic coefficients on variables.

Horizontally are listed the factors influencing these coefficients, they are grouped as follows: 1) attitude of vehicle with respect to the relative velocity: α, β; 2) angular velocities, p, q, r; and 3) control surface deflections δ_a, δ_e, δ_r.

Each "box" is now thought of to represent a functional relationship of one coefficient on one variable.

3. 3 Discussion of Dependence of the Aerodynamic Coefficients on the Variables

In a highly non-linear situation it should be realized that each of the functions which are to be thought inserted in each of the (48) boxes is a function of Mach number plus all the other variables. Each "box" would then represent a function of:

$$(M, \alpha, \beta, p, q, r, \delta_a, \delta_e, \delta_r) \tag{3.6}$$

and each of the coefficients would be one gigantic function of those 9 variables. Clearly it would be impractical to generate such functions if for no other reason than that such general aerodynamic information is unavailable.

In a purely linear situation, on the other hand, each box would only contain a derivative which is a function of M only, and a change in one of the coefficients could be expressed simply as

$$dC = \frac{\partial C}{\partial \alpha} d\alpha + \frac{\partial C}{\partial \beta} d\beta + \frac{\partial C}{\partial p} dp + \ldots\ldots \tag{3.7}$$

To make the generation of these coefficients practical without losing critical fidelity of the simulation requires a study of the aerodynamic data available, and the course of action depends strongly on the configuration of the vehicle. The result of such investigation will be a compromise between the fantastically complicated presentation of eq. (3.6) and the highly oversimplified linear one of eq. (3.7). In deciding on a method of generation of these aerodynamic characteristics it should be considered that generation techniques for functions of two or three independent variables have become practical by the method outlined in Chapter 4.

Typical aerodynamic data for the Dynasoar DS-1 glider is presented in reference 9, and more up-to-date characteristics will be available in the shortly-to-be-published reference 10. One of the most severe drawbacks of the data presented is the non-uniformity of presentation, that is, the mixed use of stability and body axes especially with regard to the moment coefficients.

4. GENERATION OF AERODYNAMIC FUNCTIONS

4.1 Introduction

An important facet of the input of aerodynamic functions into the simulator computing machinery is the mechanization of these functions. Various methods of generating functions of one variable are well known, and the technical performance of such function generators has been perfected to a high degree. In principle it is possible, through the use of an array of such one-variable function generators, to generate functions of more than one independent variable. A function of two variables, $f(x, y)$ for instance, may be presented as a family of curves $f(x, y_i)$ each member of which is considered a function of one variable: x. Using a linear interpolation between the curves (i. e., between the values y_i) a complete function $f(x, y)$ is obtained. If the function $f(x, y)$ depends upon one variable in a less non-linear fashion than upon the other, the former will, of course, be chosen to take the role of y in the above example. If, however, the function has a quite nonlinear dependence on both variables, a considerable number of curves must be generated to obtain a satisfactory representation of the function itself. This results in the necessity of generating many functions of one variable and problems arise due to the sheer number of such function generators. This situation becomes much more complex when functions of more than two independent variables are involved. It seems, however, unlikely that functions of more than three independent variables need to be generated for the aerodynamic inputs to a flight simulator computer.

A method of generating functions of two or more independent variables was referred to in a previous report on this contract (ref. 1) and was originally presented by W. Pike and T. R. Silverberg (ref. 2) in connection with the design of mechanical computers.

This method was investigated further and was found to show considerable promise. The advantages of this method are 1) even though the functions are presented by a discrete number of values, the interpolation is considerably better than a linear one; 2) the functions are continuously generated for the full range of the variables involved; and 3) an incidental advantage is that it offers an interesting method of analyzing experimental data showing frequently regularities of behavior of a function which are not apparent at first sight.

The method is outlined below, and some examples are presented which are the result of calculations made by the author during his association with the Boeing Airplane Company in the summer of 1960.

4.2 Generation of Functions of Two Variables

Consider a function of two variables, $f(x, y)$, which is defined by its discrete numerical values at all (m n) combinations of m and n selected values

of the variables x and y respectively:

$$x_1, \quad x_2 \ldots\ldots \quad x_i, \quad \ldots\ldots \quad x_m$$

$$y_1, \quad y_2 \ldots\ldots \quad y_j, \quad \ldots\ldots \quad y_n$$

The function is now symbolically written:

$$f(x_i, y_j) \equiv f_{ij}$$

Four auxiliary functions of one variable are now defined:

$$a(x_i) \equiv a_i, \quad a(x_i) \equiv \bar{a}_i$$

$$b(y_j) \equiv b_j, \quad b(y_j) \equiv \bar{b}_j$$

and these are used to represent the function f_{ij} in the following manner:

$$f_{ij} = a_i + b_j + \bar{a}_i \bar{b}_j + R'_{ij} \tag{4.1}$$

The auxiliary functions are now to be determined such that the sum of the squared errors (R'_{ij}) at the (m n) points originally selected is a minimum, i. e. ,:

$$\sum_i \sum_j (R'_{ij})^2 \quad \text{is a minimum.}$$

For the operations that follow it is necessary that the average of all the numerical values f_{ij} be zero:

$$\sum_i \sum_j f_{ij} = 0.$$

Since this is usually not the case for an arbitrary function $F(x_i, y_j)$, the function to be generated is obtained by subtracting from all F_{ij}'s their average value

$$f_{ij} = F_{ij} - \frac{1}{m\,n} \sum_i \sum_j F_{ij} = F_{ij} - F_{ij_{avg}} \tag{4.2}$$

The auxiliary functions are now obtained in the following way:

The sum-functions, a_i and b_j are found from:

$$a_i = \frac{1}{n} \sum_j f_{ij}$$

$$b_j = \frac{1}{m} \sum_i f_{ij} \tag{4.3}$$

The first residue is now computed from:

$$R_{ij} = f_{ij} - (a_i + b_j) \tag{4.4}$$

and is subsequently approximated by the product of the two product-functions:

$$R_{ij} = \bar{a}_i \bar{b}_i + R'_{ij} \tag{4.5}$$

It is necessary to calculate these product-functions by an iterative process since they are interrelated in the following manner:

$$\bar{a}_i = \frac{\sum_j [R_{ij} \bar{b}_j]}{\sum_j [(\bar{b}_j)^2]}$$

and (4.6)

$$\bar{b}_j = \frac{\sum_i [R_{ij} \bar{a}_i]}{\sum_i [(\bar{a}_i)^2]}$$

The iteration process is started by selecting an arbitrary set of m numbers to serve as an (uneducated) estimate of the $\bar{a}_i$'s. This set of numbers is indeed arbitrary, provided the numbers are not all equal. In that event, namely, the first solution of $\bar{b}_j$'s, obtained by substituting the initial estimate of the $\bar{a}_i$'s in the second of equations (4.6) will become identically equal to zero. Suggested initial estimates of $\bar{a}_i = (-1)^i$, hence an alternating of -1 and +1 or $\bar{a}_i = i$, or a counting off 1, 2, 3 .... m. *

After this selection has been made the first solution of the $\bar{b}_j$'s are found by substitution of the $\bar{a}_i$'s into the second of equations (4.6). Next the first solutions of the $\bar{b}_j$'s are substituted into the first of the equations (4.6) to yield the first solution of the $\bar{a}_i$'s. This process is now repeated, and in that way, second, third, etc., solutions of the $\bar{a}_i$'s and $\bar{b}_j$'s are obtained. Subsequent solutions of the $\bar{a}_i$'s are compared, and when they have converged to the same value, the iteration is terminated.

In the trial calculations, presented in section 4.3, it was found that the convergence to steady values of $\bar{a}_i$ and $\bar{b}_j$ is quite rapid.

---

*An interesting phenomenon is that the initial estimate of the $\bar{a}_i$'s may well affect the values to which the $\bar{a}_i$'s and $\bar{b}_j$'s will ultimately converge, it will, however, not affect their product, i.e., the values of $\bar{a}_i \bar{b}_j$.

4. 3 Result of Sample Calculations of the Generation of a Function of Two Variables

To check out the method presented above, two functions of two variables each were generated. The calculations were done by hand and, in general, carried out with slide rule accuracy.

Example 1. The first function was a typical rolling moment coefficient derivative with respect to rudder deflection, $C_{\ell_{\delta_R}}$. This coefficient is a function of Mach number, M, and angle of attack, α. The function is presented (as, for instance, faired results from wind tunnel tests) as graphs of $C_{\ell_{\delta_R}}$ vs. Mach number for various values of α as shown in fig. 3.

Now a selection is made of the (m n numerical values which are to form the rectangular matrix characterizing the function. For this case these numbers were the values of $C_{\ell_{\delta_R}}$ at all combinations of $\alpha = 0^\circ, 15^\circ, 30^\circ, 45^\circ$ and M = . 5, . 75, 1. 00, 1. 25, 1. 50. These control points are indicated also in figure 3 and correspond to the F_{ij}'s in eq. (4. 2).

Next the set is "normalized" by subtracting from each number the average value of the total set of numbers, and each number is multiplied by 10^4 to obtain more convenient numerical values; thus these values correspond to the f_{ij}'s in equation (4. 2).

The values of $a_i(\alpha)$ and $b_j(M)$ and, after the iteration process is carried out, those of $\bar{a}_i(\alpha)$ and $\bar{b}_j(M)$ are calculated by the use of equations (4. 2) and (4. 6) respectively. These values are now plotted, and a curve is faired through them resulting in graphical presentations of the functions $a(\alpha)$, $\bar{a}(\alpha)$, $b(M)$ and $\bar{b}(M)$. These functions are shown in figures 4 and 5.

Having thus obtained continuous auxiliary functions one can compute, backward as it were, the original curves, and in this way obtain an impression of the accuracy with which the generated function,

$$a(\alpha) + b(M) + \bar{a}(\alpha)\,\bar{b}(M)$$

represents the original one.

Figure 6 shows this comparison for the curves of $\alpha = 0^\circ$ and $\beta = 30^\circ$. The original control points are shown, and it is observed that at those points the curves are almost identical. The deviation of the generated curve near M = 1. 2 and $\delta = 30^\circ$ is due to improper fairing of the curves b(M) and b(M) from the six points available. This difficulty can be alleviated by either revising the fairing of these curves in fig. 5 or by selecting a large number of control points. It should be pointed out, however, that an increasingly larger number of control points does not necessarily decrease the error at the control points (residue).

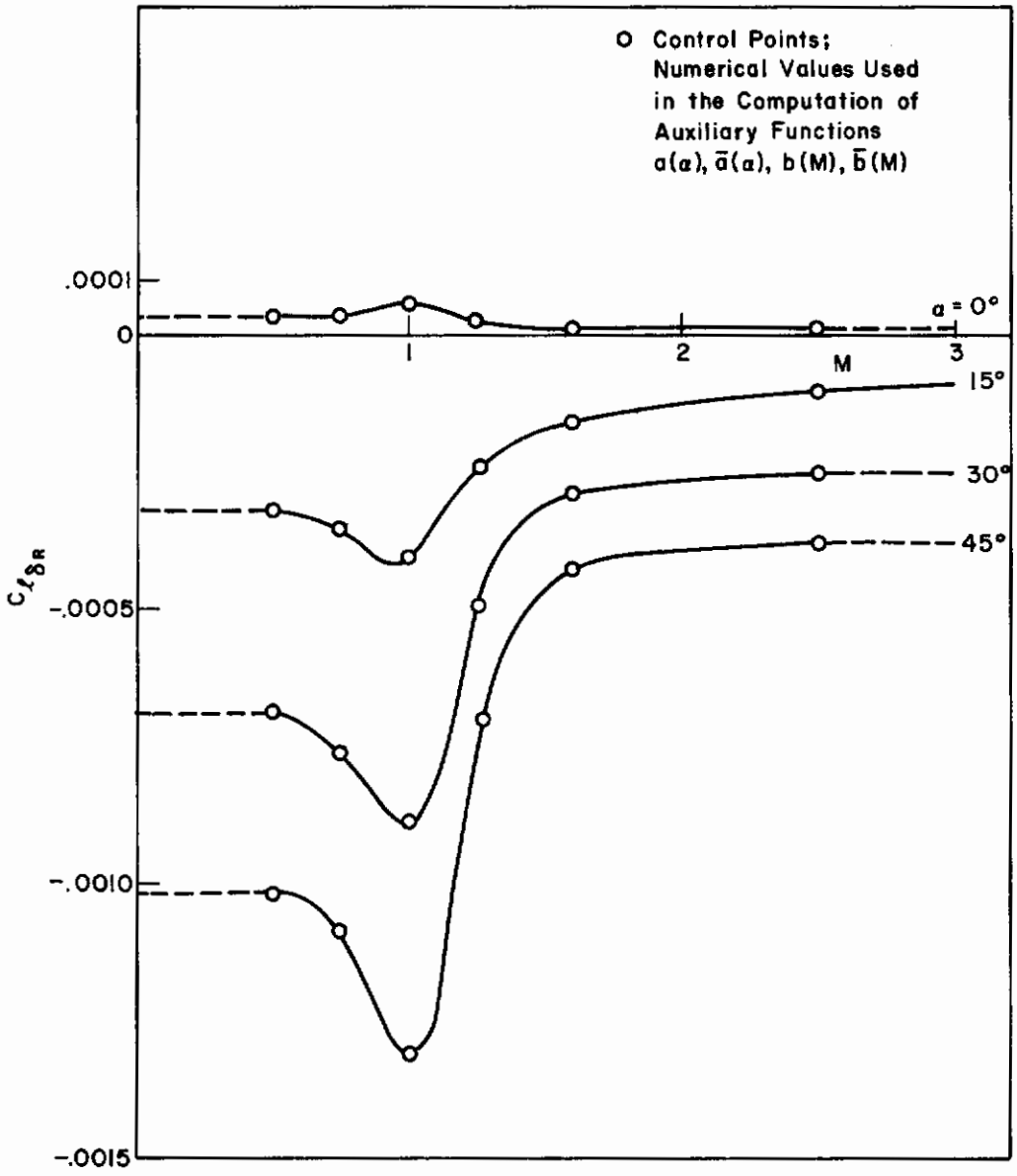

Figure 3. Typical function of two variables: $C_{\ell_{\delta_R}}$ (α, M). (See Sec. 4. 3, example 1).

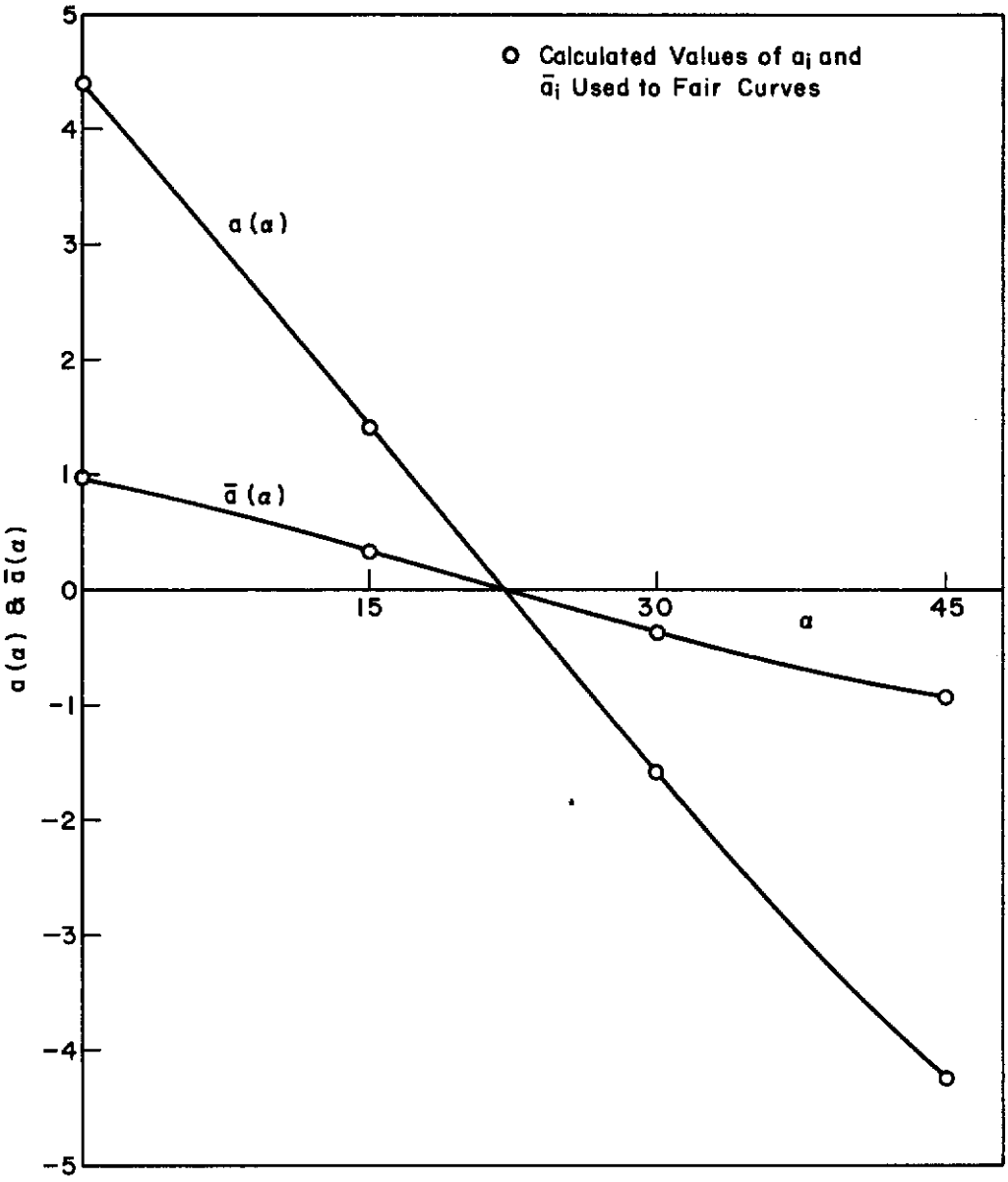

Figure 4. Auxiliary functions a (a) and $\bar{a}$ (a) used in $(C_{\ell_{\delta_R}} \times 10^4) + 4.08 = a(a) + b(M) + \bar{a}(a)\,\bar{b}(M)$. (See Sec. 4.3, example 1).

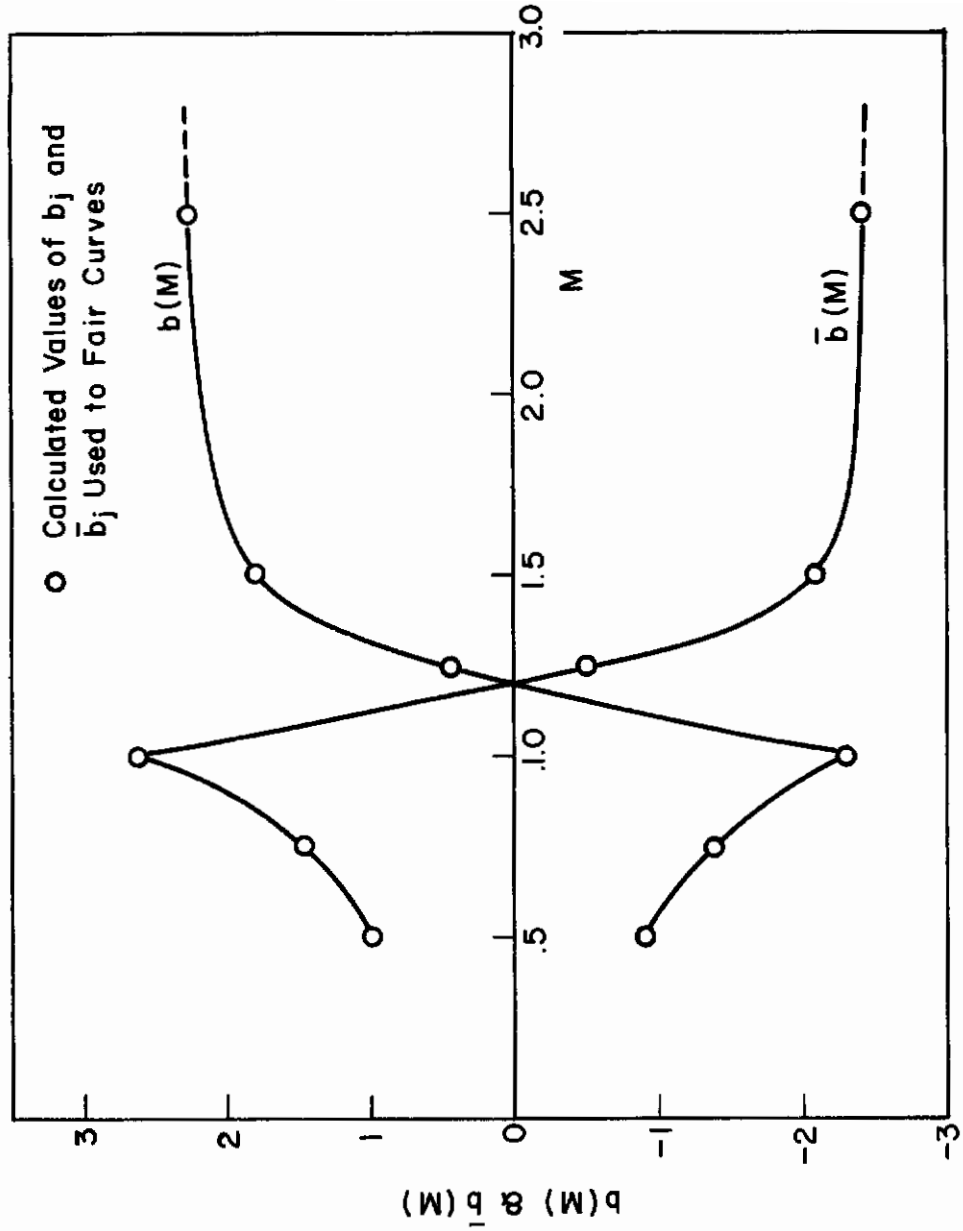

Figure 5. Auxiliary functions b(M) and $\bar{b}(M)$ used in $(C_{\ell_{\delta_R}} \times 10^4) + 4.08 = a(\alpha) + b(M) + \bar{a}(\alpha)\,\bar{b}(M)$. (See Sec. 4.3, example 1).

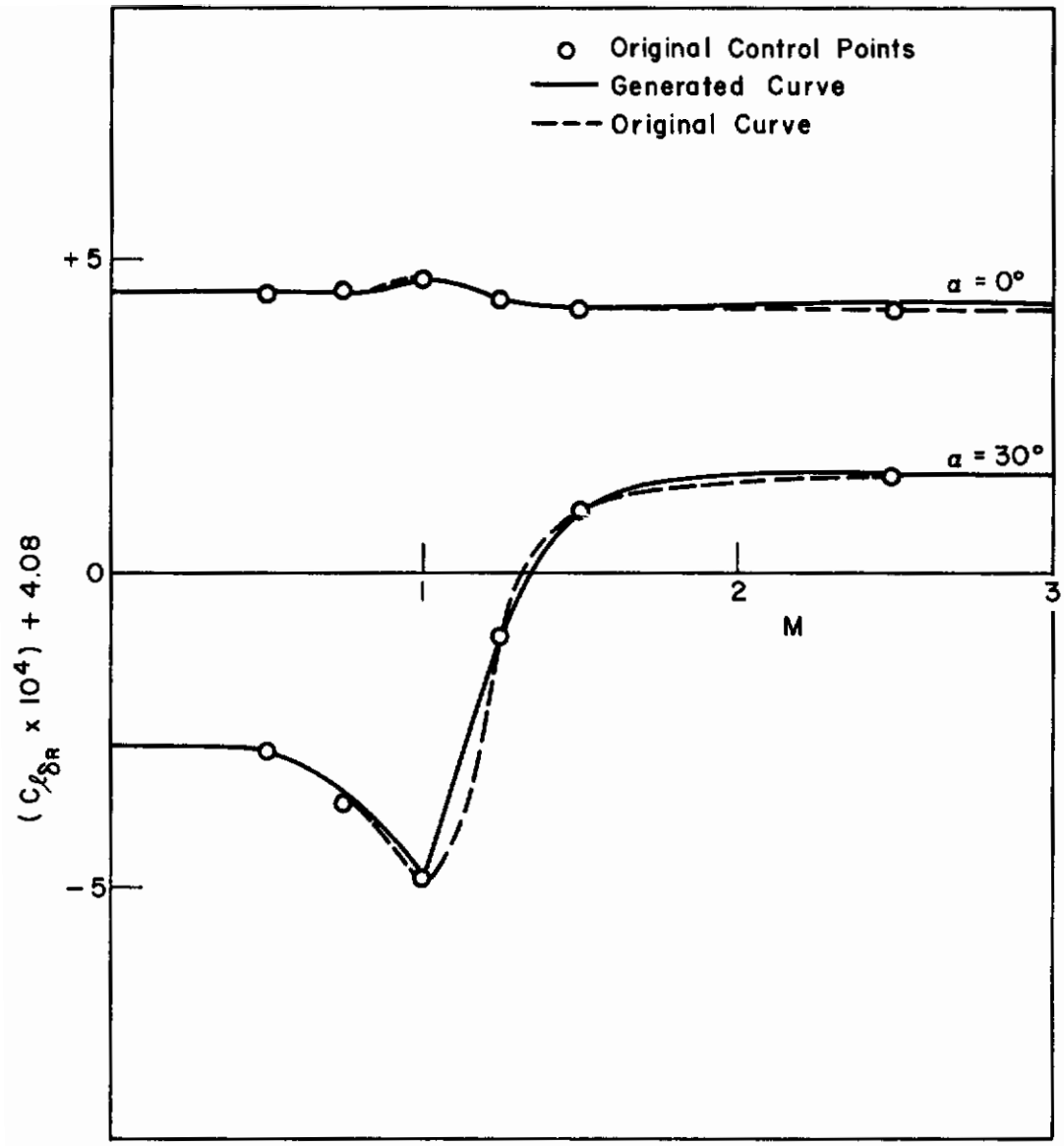

Figure 6. Comparison of Generated Curves with Original Data: $C_{\ell_{\delta_R}}$ (normalized) vs. M for $\alpha = 0^\circ, 30^\circ$.

This particular example demonstrates another facet of this method. It shows that $a(\alpha)$ and $\bar{a}(\alpha)$ are almost straight lines. Approximating them by straight lines makes the use of function generators for these two functions unnecessary. Also a remarkable similarity shows up in the functions $b(M)$ and $\bar{b}(M)$. Here it seems that the function $b(M)$ can be approximated by

$$\bar{b}(M) = - (\text{const.})\ b(M)$$

so that these two functions require only one function generator. In fact, the entire function $C_{\ell_{\delta_R}}(\alpha, M)$ requires only one function generator.

Example 2. The second example was selected because it was less regular in appearance. The function is a typical aerodynamic pitching moment coefficient as a function of elevator deflection, δ_e, and angle of attack, α.

Here, control points were chosen at all combinations of $\delta_e = -45^o$, -20^o, 0^o, $+10^o$, $+20^o$ and $\alpha = 0^o$, 10^o, 20^o, 30^o, 45^o. The "normalized" function is shown in fig. 7 , and the control points were not selected at values of $\delta_e = -30^o$, -10^o, and $+30^o$.

The auxiliary functions $a(\delta_e)$, $\bar{a}(\delta_e)$, $b(\alpha)$ and $\bar{b}(\alpha)$ are shown in figures 8 and 9.

Figure 10 shows the comparison of the generated functions with the original ones for $\delta_e = -45^o$, 0^o, $+20^o$.

In order to check the interpolation ability of the method, the generated curves for $\delta_e = -30^o$, -10^o, and $+30^o$ are compared with the original curves in fig. 11. It should be realized here, that altogether no control points were selected on these curves. Note the excellent agreement for $\delta_e = -30^o$ and -10^o. The curves for $\delta_e = +30$ was extrapolated rather than interpolated and, as a consequence, shows a poor fit.

As in the first example, it appears here that the curves $a(\delta_e)$ and $\bar{a}(\delta_e)$ may be related in a manner such as:

$$\bar{a}(\delta_e) = K_1\ [\, a(\delta_e) + K_2 \,]$$

where K_1 and K_2 are constants. In this fashion one function generator may serve for both functions.

Short cuts of this nature cannot be generalized but must be investigated for each case separately.

4. 4 Generation of Functions of Three Variables

The method presented in ref. 2 is there extended also to functions having N independent variables. Since the number of auxiliary functions of one variable

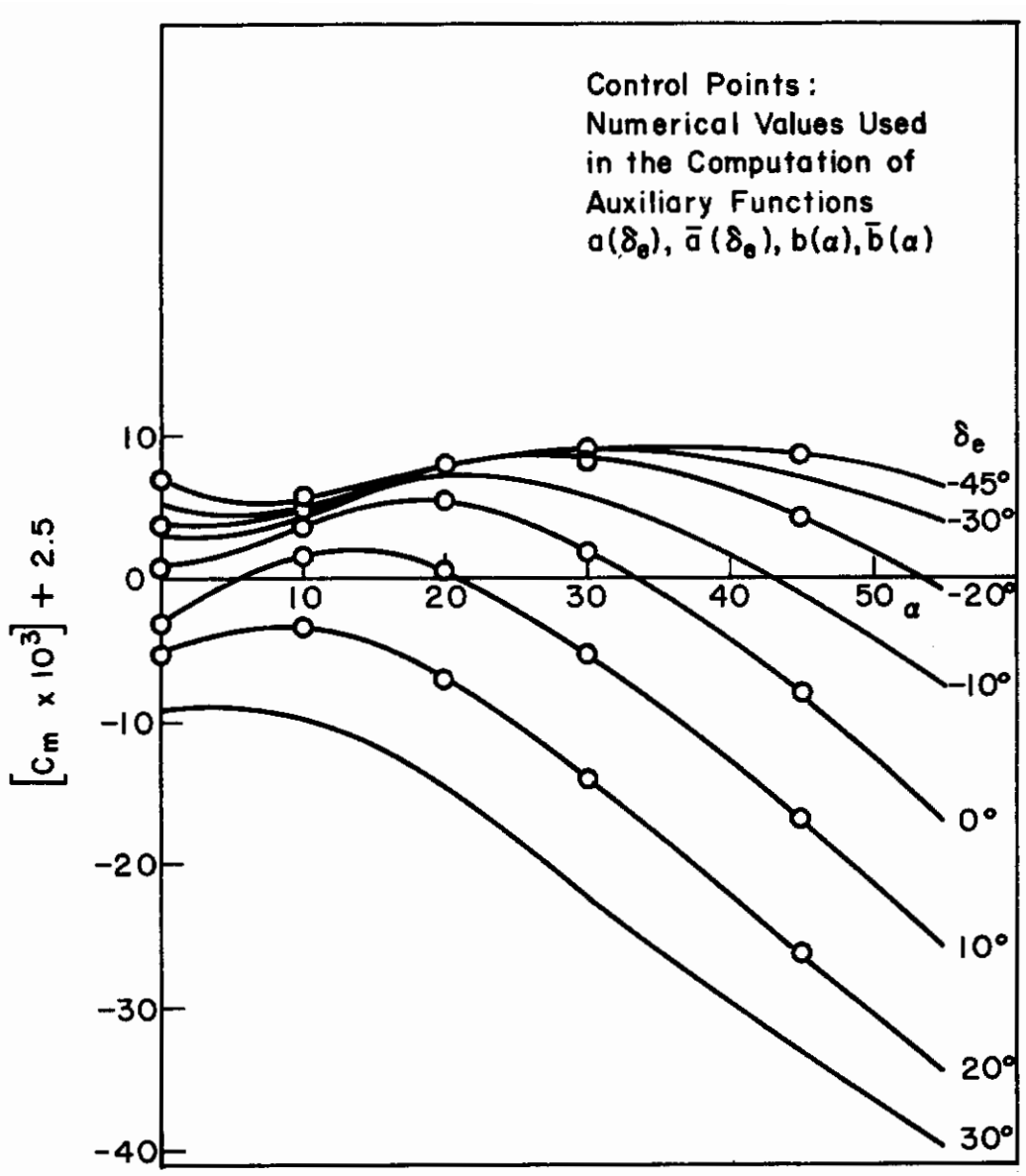

Figure 7. Typical functions of two variables: C_m (δ_e, α) normalized. (See Sec 4. 3, example 2).

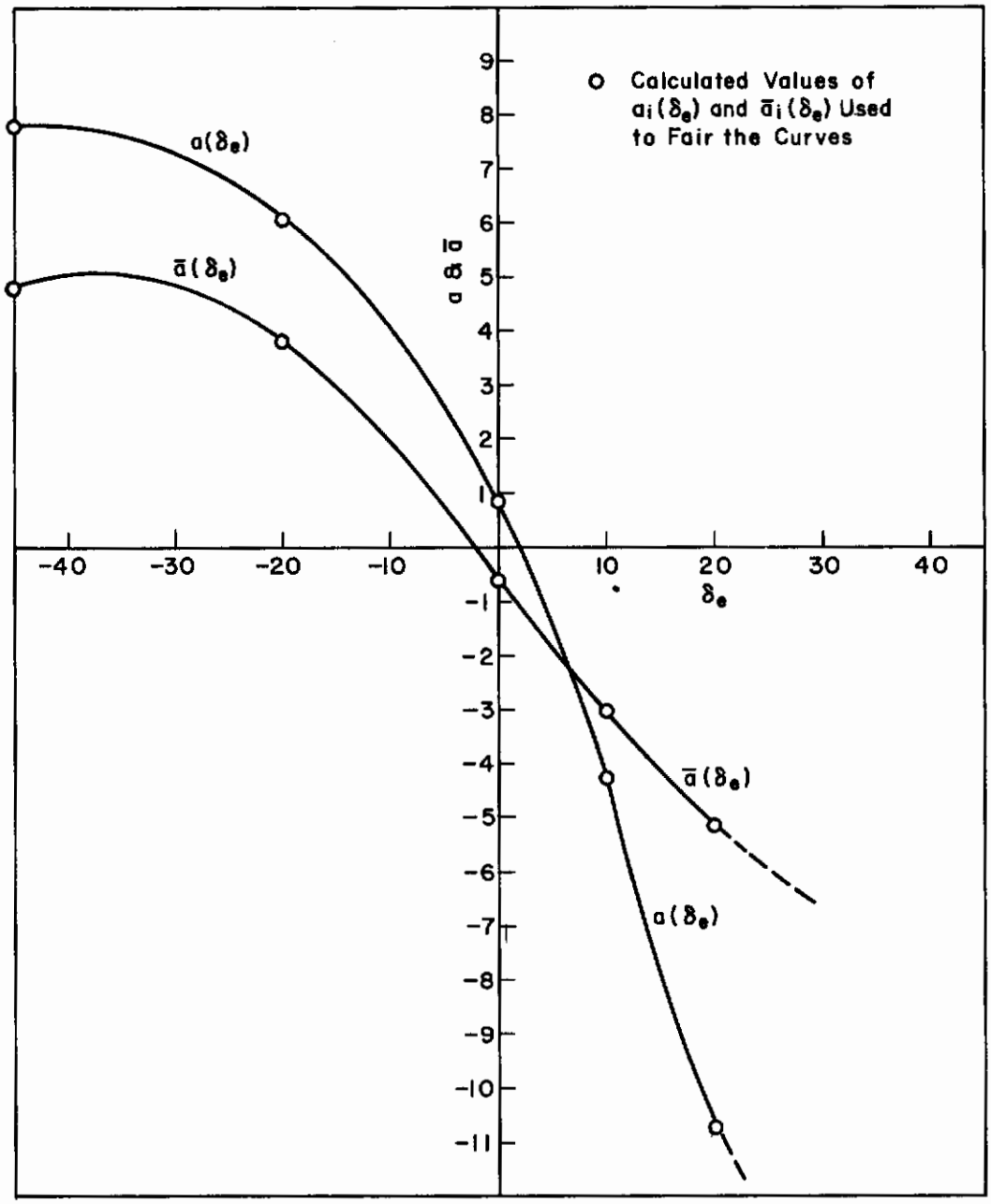

Figure 8. Auxiliary functions $a(\delta_e)$ and $\bar{a}(\delta_e)$ used in $(C_m \times 10^3) + 2.5 = a(\delta_e) + b(a) + \bar{a}(\delta_e)\,\bar{b}(a)$. (See Sec. 4.3, example 2).

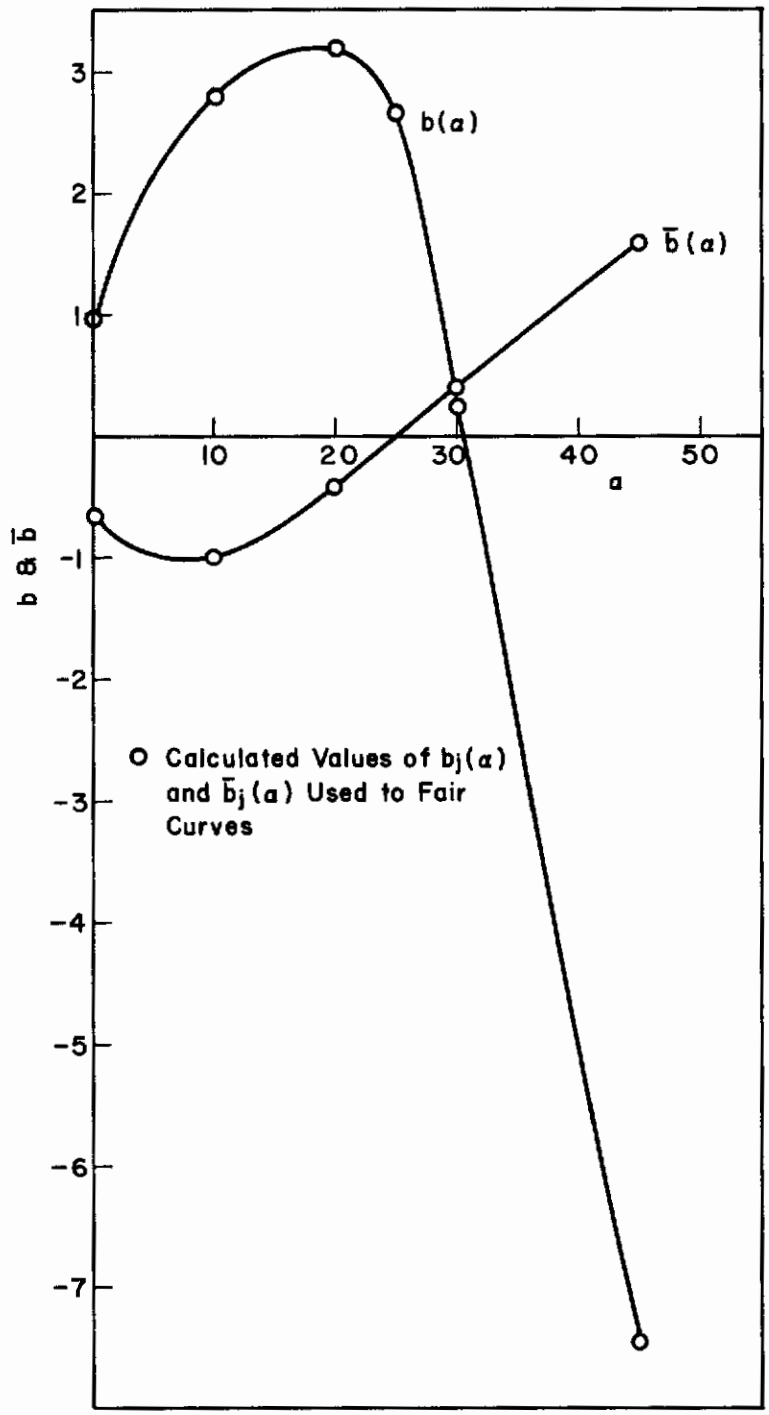

Figure 9. Auxiliary Functions b(a) and $\bar{b}(a)$ Used in $(C_m \times 10^3) + 2.5 = a(\delta_e) + b(a) + \bar{a}(\delta_e)\,\bar{b}(a)$. (See Sec. 4.3, example 2).

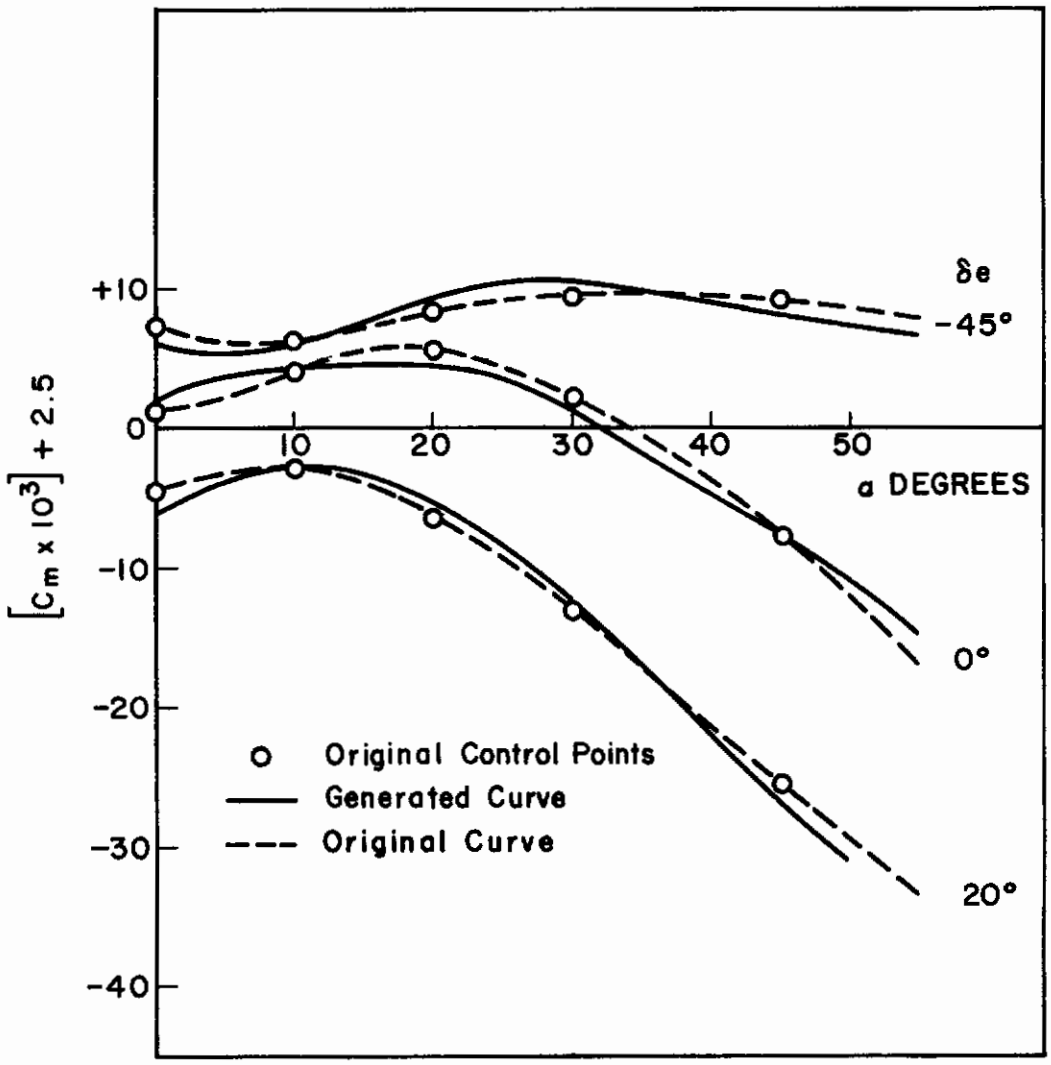

Figure 10. Comparison of generated curves with original data: C_m (normalized) vs. α for δ_e = -45°, 0°, +20°.

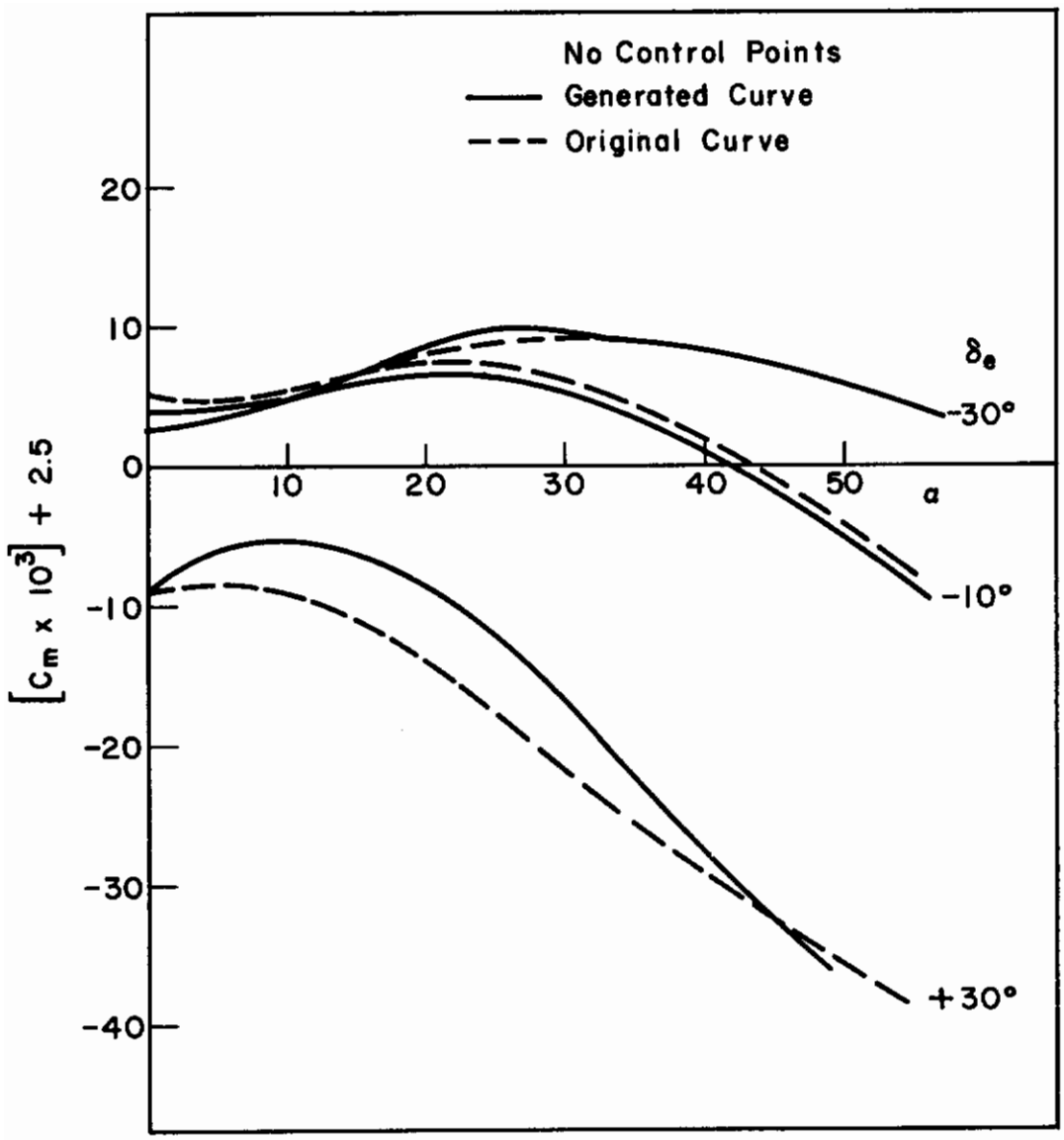

Figure 11. Comparison of generated curves with original data: C_m (normalized) vs. α for $\delta_e = -30^o, 0^o, +30^o$.

increases as the square of N and since there is no anticipation for a need to generate functions of more than three variables, the procedure for calculating the auxiliary functions for the case N = 3 is outlined below.

Let a function of three variables, assumed to be already normalized, $f(x, y, z)$, be defined by its numerical values at all (m n p) combinations of

$$x_1, \quad x_2, \quad \ldots\ldots\ldots \quad x_m$$

$$y_1, \quad y_2, \quad \ldots\ldots\ldots \quad y_n$$

$$z_1, \quad z_2, \quad \ldots\ldots\ldots \quad z_p$$

or, symbolically,:

$$f(x_i, y_j, z_k) = f_{ijk}$$

This function is now approximated by the sum of

1) three sum-functions, f_i, f_j, f_k (functions of x_i, y_j, z_k respectively), and
2) three two-variable functions F_{ij}, F_{jk}, F_{ki} (functions of (x_i, y_j), (y_j, z_k), and (z_k, x_i) respectively).

The sum functions are defined by:

$$f_i = \frac{1}{n\,p} \sum_j \sum_k f_{ijk}$$

$$f_j = \frac{1}{p\,m} \sum_k \sum_i f_{ijk} \qquad (4.7)$$

$$f_k = \frac{1}{m\,n} \sum_i \sum_j f_{ijk}$$

The first residue, R_{ijk}, defined by:

$$R_{ijk} = f_{ijk} - [f_i + f_j + f_k] \qquad (4.8)$$

is approximated by the sum of the three two-variable functions:

$$R_{ijk} = F_{ij} + F_{jk} + F_{ki} \qquad (4.9)$$

where these functions are defined by:

$$F_{ij} = \frac{1}{p} \sum_k R_{ijk}$$

$$F_{jk} = \frac{1}{m} \sum_i R_{ijk} \qquad (4.10)$$

$$F_{ki} = \frac{1}{n} \sum_j R_{ijk}$$

Each of these functions can now be treated in the same manner as discussed in the previous section. Each function will thus be replaced by two sum-functions, which eventually may be combined with the one-variable functions of equation (4. 7), and a term consisting of the product of the product-functions. In this manner it can be verified that, at worst, nine one-variable functions will need to be generated as auxiliary functions.

4. 5 Additional Comments

The calculations involved to obtain the auxiliary functions needed (especially the product functions since they involve an iteration process) are quite lengthy and suggest the design of a digital computer program to perform those calculations.

Such a program has been set up by the Boeing Airplane Company and has been applied to several functions of two variables using a much larger number of control points than was possible in the hand calculations above. The results are reported in an unpublished paper (ref. 3) by Parente and Moshier. The generated curves were indistinguishable from the original ones.

The above digital program has been extended, in slightly modified form, to include functions of three independent variables.

BIBLIOGRAPHY

1. Isakson, G., and H. Buning, "A Study of Problems in the Flight Simulation of VTOL Aircraft," The University of Michigan, WADC Technical Note 59-305, Wright Air Development Center, Wright-Patterson Air Force Base, Ohio.

2. Pike, E. W. and T. R. Silverberg, "Designing Mechanical Computers." Part I. "Functions Having Two Variables," Machine Design, July 1952; Part II. "Functions Having More Than Two Independent Variables," Machine Design, August 1952.

3. Parente, F. J. and C. P. Moshier, "Application of Multivariable Function Generation Techniques to Electronic Analog Computers," Boeing Airplane Company, Seattle, Washington, (unpublished paper).

4. Eggleston, J. M., S. Baron, and D. C. Cheatham, "Fixed Base Simulation Study of a Pilot's Ability to Control a Winged Satellite Vehicle During High Drag Variable Lift Entries," NASA TN D-228, National Aeronautics and Space Administration, 1960.

5. Minzner, R. A. and W. S. Ripley, "The ARDC Model Atmosphere, 1956," AFCRC TN-56-204, U. S. Air Force Cambridge Research Center, Cambridge, Massachusetts, December 1956.

6. Truitt, R. W., Hypersonic Aerodynamics, The Ronald Press Company, New York, 1959.

7. Hendrikson, C. H., "Newtonian Aerodynamics Applied to Representative Reentry Bodies," Boeing Airplane Company, Seattle, Washington, Document No. D7-2505.

8. Howe, R. M., "An Investigation of Flight Equation Requirements for Simulators of Aircraft Up to Mach 3. 5," Department of Aeronautical Engineering, The University of Michigan, WADC Technical Note 57-144, Wright Air Development Center, Wright-Patterson Air Force Base, Ohio, March 1957.

9. "Aerodynamic Stability and Control Data; Glider Model 844-2050," (unclassified title), Boeing Airplane Company, Seattle, Washington, Document 2-800065, (Confidential).

10. "DS-I Aerodynamics Report - Glider Stability and Control," (unclassified title), Boeing Airplane Company, Seattle, Washington, Document No. D5-4399-2, (Confidential).